The Open Civil Engineering Journal

Content list available at: https://opencivilengineeringjournal.com

RESEARCH ARTICLE

Application of ANN Predictive Model for the Design of Batch Adsorbers - Equilibrium Simulation of Cr(VI) Adsorption onto Activated Carbon

Clint Sutherland[1,*], Beverly S. Chittoo[1] and Chintanapalli Venkobachar[2]

[1]*Unit for Project Management and Civil Infrastructure Systems, The University of Trinidad and Tobago, San Fernando Campus, Arima, Trinidad and Tobago*

[2]*Department of Civil and Environmental Engineering, The University of the West Indies, Saint Augustine, Trinidad and Tobago (WI)*

Abstract:

Background:

Escalation of industrial processes continues to increase the concentrations of Cr(VI) in wastewater above permissible discharge limits. Persistent exposure to Cr(VI)may result in deleterious effects on human health, aquatic life, and the environment. Laboratory-scale adsorption studies have proven effective in achieving the low treatment levels demanded by statutory authorities. The eventual design of the pilot and full-scale systems hinges on the ability to predict adsorption behavior mathematically.

Objective:

The objective of this study is to elucidate the mechanism of Cr(VI) adsorption and to develop an Artificial Neural Network (ANN) model capable of accurately simulating complex multi-layered adsorption processes.

Methods:

Batch equilibrium experiments were conducted for the removal of Cr(VI) by activated carbon. Conventional two and three-parameter equilibrium models such as the Langmuir, Freundlich, Sips, original BET and modified BET were used to simulate the data and expound the mechanism of adsorption. An ANN model was constructed with the built-in effect of the residual Cr(VI) concentration for the prediction of the equilibrium sorption capacity.

Results:

The modified BET model was most successful at predicting the monolayer coverage. However, the model failed to capture the complex shape of the isotherm at higher initial concentrations. The highest correlation to the equilibrium data was revealed by the ANN model ($R^2 = 0.9984$).

Conclusion:

A batch adsorber was successfully designed using mass balance, and incorporating the predictive ability of the ANN model. In spite of the ANN's ability to simulate the adsorption process, it provides little insight into the mechanism of adsorption. However, its ability to accurately predict Cr(VI) removal enables the up-scaling of the adsorption processes to pilot and full-scale design.

Keywords: Activated Carbon, Chromium (VI), Equilibrium, Adsorption, Artificial Neural Network, Batch Adsorber.

Article History	Received: March 05, 2019	Revised: May 18, 2019	Accepted: May 30, 2019

1. INTRODUCTION

Chromium is a priority pollutant and exists in various oxidative forms. However, from an environmental pollution point of view, the hexavalent state, Cr(VI), in the forms of chromate (CrO_4^{2-}), dichromate (CrO_7^{2-}), and chromium oxide (CrO_3) is considered the most toxic state of chromium, due to its high oxidizing potential, high solubility, and mobility across the membranes in living organisms and in the environment [1]. According to Thambavani and Kavitha [2], persistent exposure to Cr(VI) affects human health by causing cancer in the digestive tract and lungs, and other health problems such as skin dermatitis, bronchitis, perforation of the nasal septum, severe diarrhea, and hemorrhaging. Additionally, Cr(VI) is

* Address correspondence to the author at the Unit for Project Management and Civil Infrastructure Systems, The University of Trinidad and Tobago, San Fernando Campus, Arima, Trinidad and Tobago; Tel: +18684975744; Fax: +18682231621; E-mail: clint.sutherland@utt.edu.tt

toxic to many plants, animals, and microorganisms in the aquatic environment [3]. The extensive use of Cr(VI)in industrial processes such as electroplating, tanning, textile dyeing, and wood preserving invariably results in the discharge of effluents containing soluble Cr(VI) in concentrations above permissible levels [4, 5]. Mubeena and Muthuraman [6] reported Cr(VI)concentrations of 10.0 mg/L in industrial electroplating effluents while Mishra and Soni [7] reported Cr(VI)concentrations as high as 6.7 mg/L in effluents from dyeing and printing industries functioning in Balotara, India. Tara *et al.* [8] reported 9.67 mg/L of Cr(VI)in textile effluent obtained from industry in Faisalabad, Pakistan. World Health Organization (WHO) recommends that the level of Cr(VI) in wastewater be regulated below 0.05 mg/L [9]. Thus, research into the removal of Cr(VI)from wastewater is critical to protecting human health and the environment.

Some of the primary treatment methods adopted for industrial-scaled remediation of such metal ions are ion exchange, chemical precipitation, and adsorption [10]. Due to its ability to attain low concentration levels, insensitivity to toxic pollutants and simplicity of design and operation, adsorption research has become a major topic of academic focus. Researchers have studied various natural and synthetic adsorbents with each shown to possess a varying affinity for Cr(VI) ions. Goswami and Ghosh [11], reported a monolayer sorption capacity of 3.48 mg Cr(VI) ions per g of synthetic hydrous stannic oxide. Alemu *et al.* [12] investigated the potential of vesicular basalt for Cr(VI) sorption. The maximum sorption capacity was 79.20 mg/kg of the adsorbent. Agroindustrial waste such as grape and olive waste attained capacities for Cr(VI) of 108.12 mg/g and 100.47 mg/g, respectively [13]. Reddy *et al.* [14] studied the removal of Cr(VI) using mustard oil cake. The authors reported a total chromium removal of 29 mg/g. Living and dead cells of *Bacillus coagulans* successfully biosorbed 23.8 and 39.9 mg Cr/g dry weight, respectively of Cr(VI) ions [15]. While biomass waste material-derived activated carbon successfully removed 73.1 mg/g Cr(VI) [16].

The fitting of experimental data to equilibrium models can provide valuable insights into the mechanisms of adsorption and the economic feasibility of the sorbent's commercial application to enable optimization of the design and up-scale of adsorption units [17, 18]. However, the accuracy of the simulation cannot be overemphasized, as an accurate prediction of the sorption process is critical to enable advancement to pilot and full-scale design. However, in many reported instances, isotherms produced by Cr(VI) adsorption exhibits the BET Type II and Type IV [19] or the Giles L-shape [20] isotherm. Such observations have been reported by Netzahuatl-Muñoz *et al.* [21] for the sorption of Cr(VI) onto Cupressus lusitanica bark; Terangpi *et al.* [22] for the removal of Cr(VI) by a modified aniline formaldehyde condensate polymer; Sfaksi *et al.* [23] for the removal of Cr(VI) by cork waste; Rossi *et al.* [24] for the removal of Cr(VI) by chemically treated Saccharomyces cerevisiae biomass. Similar complex isotherms have been reported for other adsorbates and adsorbents as methylene blue removal by activated sunflowers seeds shell carbon [25], dazomet adsorption by zoelite [26], and p-nitrophenol adsorption through N_2-thermal-based treatment of activated carbons [27].

Zhang *et al*. [28] studied the adsorption of Cr(VI) onto carbon-microsilica composites. The authors concluded that their complex shaped isotherm belongs to subgroup 3 of L-shape isotherm which corresponds to the classification of Giles *et al*. [20]. They went on to explain that this shape indicates the formation of a second layer due to an abound of oxygen functional groups, such as hydroxyl, carboxyl and sulfonic groups being introduced into the surface which form H-bond with $HCrO_4^-$ radical at an acid aqueous solution and remove Cr(VI) from the aqueous solution. When all of the available monolayer sites are occupied, the $HCrO_4^-$ radical in solution could also be adsorbed by H-bond between the $HCrO_4^-$ radical in solution and the $HCrO_4^-$ radical adsorbed on the adsorbent. Ramadoss and Subramaniam [29] reported on the adsorption of Cr(VI) onto blue-green algae. The authors conducted a critical review of isotherm models to simulate the obtained L-shape isotherm. The study considered 12 two-parameter isotherm models including Langmuir [30], Freundlich [31], Jossens [32], Fowler-Guggenheim [33], and Temkin [34]; 18 three-parameter models including the Redlich-Peterson isotherm [35], Radke-prausnitz [36], Koble-Corrigan [37], Toth [38], Sips [39], and Khan [40]; 4 four-parameter models, namely the Baudu Isotherm Model [41] and the Weber-van Vliet Isotherm Model [42]; and the Fritz-Schlunder [43] five-parameter model. The highest R^2 (0.9919) to the experimental data was produced by the three-parameter Koble-Corrigan isotherm model, however, the authors concluded that the model was incapable of defining the experimental data. Pedroza *et al*. [44] also studied the adsorption of Cr(VI) from synthetic solution. In their findings for adsorption using blast furnace dust, the resulting experimental isotherm exhibited a similar complex shape, *i.e.* an initial plateau followed by a sudden rise in the curve at higher aqueous concentration. The Freundlich isotherm produced the highest R^2 (0.96), however, in this instance, the non-linear plot revealed that the correlation falls off as the curve transitions from monolayer to multilayer adsorption. In the study by Schneider *et al*. [45] of phosphate removal using nanostructured ZnFeZr oxyhydroxide precipitate, the BET model represented the reaction well at higher initial concentrations however, the correlation fell off at lower concentrations. A similar shortfall in the use of conventional models was also observed in work by Al-Qodah and Shawabkah [46] for the adsorption of triadimenol pesticide using activated carbon.

ANN is a computational technique derived from the biological counterparts and based on the concept that a highly interconnected system of simple processing elements known as nodes or neurons enables the learning of highly complex nonlinear interrelationships existing between input and output variables of the data-set [47]. The first artificial neuron was produced in 1943 by McCulloch and Pits [48]. This technique has since gained considerable applications primarily towards the development of predictive models to forecast future values of a particular response variable from a given set of independent variables [49]. Such predictive models are information-driven models and do not require assumptions about the input distribution [50]. Further, it benefits not only in saving cost and time required for experimental studies but also in improving the efficient application of full-scale adsorption

systems [51]. Over the years, ANN has also been successfully used to model foundation settlement [52], analysis of airfield pavement heavy-weight deflectometer data [53], batch and column adsorption processes [54 - 58], fermentation [59] and air drying [60].

The need to attain an accurate mathematical simulation of complex adsorption isotherms provides sufficient interest to undertake this study. Activated carbon remains the most popular adsorbent and has been used with great industrial success [61]. Consequently, research into the removal of Cr(VI) by activated carbon continues unabated. Batch equilibrium studies were conducted using commercial activated carbon to adsorb Cr(VI) ions from aqueous solution. The intent is to subsequently incorporate the operational parameters of the adsorption isotherm into an ANN and develop a predictive model. Using mass transfer, the predictive model may be used to overcome isotherm complexities and facilitate accurate process design and up-scaling. The use of ANN to overcome the shortcomings of conventional fundamental models have been successfully applied by researchers such as Gomez *et al.* [62] for the simulation of column breakthrough curves; Lee *et al.* [63] for the design of full-scale coke-plant wastewater treatment process; and Hussain *et al.* [64] for the prediction of porosity in foods during drying.

The objectives of this work are: (1) to describe the process of Cr(VI)adsorption onto activated carbon through batch equilibrium studies; (2) to elucidate the mechanisms of adsorption aided by simulation using isotherm models; (3) to develop a predictive model using a back-propagation artificial neural network to accurately simulate Cr(VI) adsorption onto activated carbon; and (4) to use the ANN predicted adsorption capacity to design batch adsorbers.

2. EXPERIMENTAL

2.1. Adsorbent

The granular activated carbon used in these experiments was Calgon Filtrasorb 300. According to the manufacturer Calgon Corp. Canada, this carbon has an iodine number of 900 mg/g, an intrinsic pore volume of 0.85 and a BET surface area of 950-1050 m^2/g. The carbon was crushed and sieved to produce a Geometric Mean Size (GMS) of 0.21 mm. The (GMS) is expressed as (diameter of upper sieve × diameter of lower sieve)$^{0.5}$ [65].

2.2. Adsorbate

Reaction solutions were prepared using potassium chromate diluted in distilled water (prepared by a Corning Mega-Pure System MP-1) of pH approximately 7 and conductivity < 5 μmhos/cm. Solution pH was then adjusted to 2.5 using appropriate solutions of HCl which was previously determined to be optimum [66]. Solution pH was measured by a pH meter (Accumet Research-AR10, Fisher Scientific). Cr(VI) concentrations were determined by an Atomic Adsorption Spectrophotometer (Perkin-Elmer 3030B).

2.3. Experimental Procedure

2.3.1. Equilibrium Studies

Batch adsorption studies were conducted using the parallel method according to EPA OPPTS method 835.1230 [67]. The equilibrium experiments were conducted with the initial Cr(VI) metal ion concentration of 66 mg/L held constant while the adsorbent concentration was varied. Adsorbent dose was varied from 0.5 to 5 g/L for contact times of 60 minutes. The adsorbent was then separated by using Whatman No. 2 qualitative filter paper. The concentration of metal ions on activated carbon at the corresponding equilibrium conditions was determined using the mass balance equation expressed as follows:

$$q_e = \frac{(C_o - C_e)}{M} \times V \quad \textbf{(1)}$$

Where, q_e (mg/g) is the mass of the adsorbate adsorbed per mass of adsorbent, C_o (mg/L) is the initial adsorbate concentration in solution, C_e (mg/L) is the final adsorbate concentration in solution, V is the volume of synthetic adsorbate solution, and M (g) is the mass of the adsorbent.

2.3.2. Equilibrium Models

2.3.2.1. Langmuir Isotherm

The Langmuir isotherm assumes that adsorption sites on the adsorbent possess an equal affinity for molecules and that each site is capable of adsorbing one molecule thus forming a monolayer [30]. The model is represented as follows:

$$q_e = \frac{q_m K_L C_e}{1 + K_L C_e} \quad \textbf{(2)}$$

Where, q_m (mg/g) is the maximum specific uptake, K_L (L/mg) is the Langmuir's constant related to the apparent heat change.

2.3.2.2. Freundlich Isotherm

Firth as cited in [68], explained that the equation of the form $x = kc^{1/n}$ was first applied to adsorption of gases by De Saussure in 1814. Its application was further extended to solutions by Boedecker in 1859 [68]. In 1906, Freundlich described the adsorption isotherm mathematically as a special case for non-ideal and reversible adsorption [31]. This equation is presented as:

$$q_e = K_F C_e^{1/n} \quad \textbf{(3)}$$

Where, K_F is the Freundlich constant, and n is the Freundlich exponent.

2.3.2.3. Sips Isotherm

Sips [39] developed an empirical sorption isotherm which assumes a molecule can occupy two sites also called the Langmuir-Freundlich isotherm:

$$q_e = \frac{q_S (a_S C_e)^{n_S}}{1 + (a_S C_e)^{n_S}} \quad \textbf{(4)}$$

Where, C_e (mg/L) is the final concentration of ions in solution, q_s (mg/g) is the equilibrium sorption capacity, α_s is the

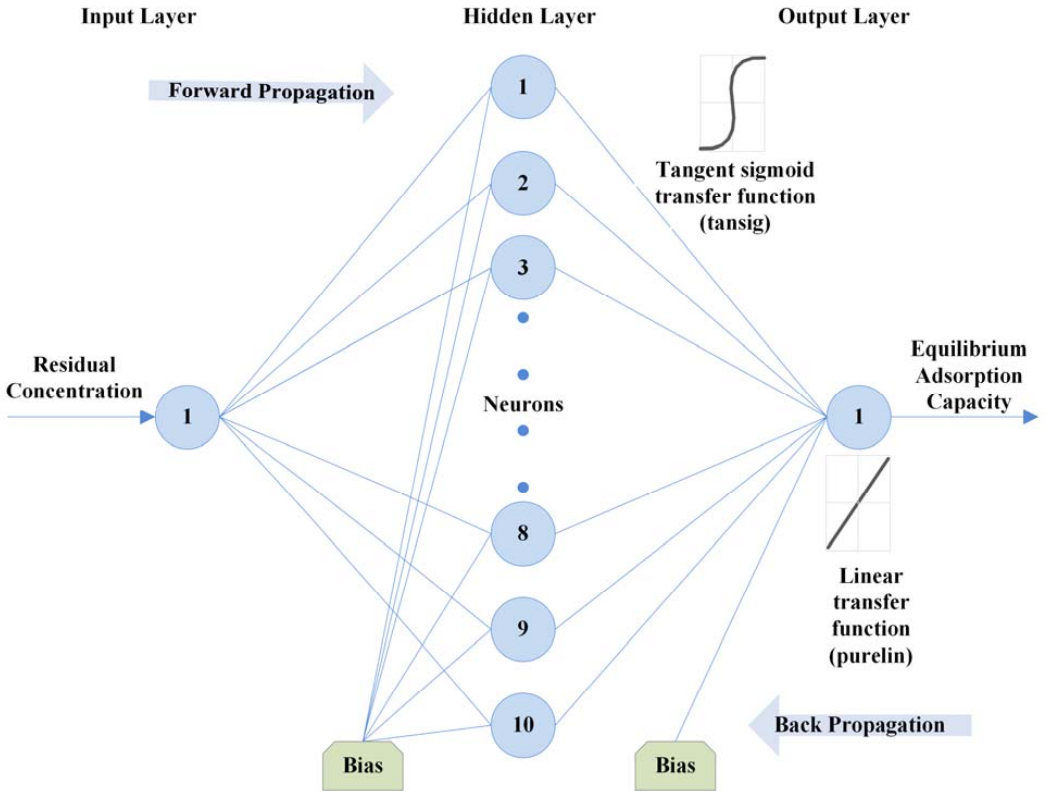

Fig. (1). Structure of ANN model.

affinity constant for adsorption, and n_s is the index of heterogeneity.

2.3.2.4. Original BET Isotherm (Type 1)

The BET isotherm is an S-shape isotherm originally developed for gas adsorption [69]. According to Ebadi *et al*. [70], the model allows the determination of multilayer adsorption behavior, monolayer adsorption capacity and heat of adsorption at various adsorption layers. When applying the BET equation to liquid phase adsorption the liquid phase concentration, C is simply substituted for the partial pressure. However, difficulty arises in replacing the saturation partial pressure with the corresponding term in the liquid phase. The application of the model has varied among researchers, where a number of researchers have used C_S, as an adjustable parameter and have calculated it by fitting the BET isotherm equation to the experimental data [70]. This form of the model referred to here as BET Type 1 has three degrees of freedom which can be solved by non-linear regression and is given by:

$$q_e = \frac{q_{mBET1} K_b \frac{C_e}{C_S}}{\left(1-\frac{C_e}{C_S}\right)\left(1-\frac{C_e}{C_S}+K_b\frac{C_e}{C_S}\right)} \quad (5)$$

Where, q_e (mg/g) is the amount of adsorbate sorbed on the solid surface, q_m (mg/g) is the amount of adsorbate corresponding to complete monolayer adsorption, K_b is the constant expressive of energy of interaction with the surface, C_e (mg/L) is the equilibrium liquid phase concentration, and C_S (mg/L) is an adjustable parameter related to the liquid phase saturated concentration.

2.3.2.5. Modified BET Isotherm (Type 2)

Ebadi *et al*. [70] presented an adjusted form of the BET isotherm (BET Type 2) for liquid phase where the saturation concentration of the adsorbate was eliminated from the classical BET isotherm equation, and the equilibrium constant of adsorption of upper layers (K_L) was reinstated in the equation. The adjusted form of the model is given by:

$$q_e = \frac{q_{m(BET2)} K_S C_{eq}}{(1-K_L C_{eq})(1-K_L C_{eq}+K_S C_{eq})} \quad (6)$$

Where, q_{mBET2} (mg/g) is the amount of adsorbate corresponding to complete monolayer adsorption, K_L $(mg/L)^{-1}$ is the equilibrium constant of adsorption for upper layers in BET isotherm, K_S $(mg/L)^{-1}$ is the equilibrium constant of adsorption for the first layer in Langmuir and BET isotherms and C_{eq} (mg/L) is the equilibrium liquid phase concentration.

2.3.3. Theory of Artificial Neural Network

An artificial neural network (ANN) attempts to mimic how a biological system functions and how they can be utilized for their novel architecture to solve highly complex, undefined and nonlinear mathematical problems [71]. In this study, the

multilayer feed-forward neural network trained by backpropagation is adopted. This ANN architecture is formed by the number of layers, number of neurons in different layers, transfer function and initial weights which interconnect each layer. According to Lek and Guegan [72], the non-linear elements (neurons) are arranged in successive layers and the information flows unidirectional, from input layer to output layer, through the hidden layers (Fig. **1**). The input values (C_e within the range of 5.6 to 52.8 mg/L) are weighted before entering the hidden layer while the bias units add a constant term in the weighted sum, which improves convergence. The output is based on the sum of the weighted values from the input layer and modified by a transfer function [66]. After the network's output is compared with the target vector (q_e within the range of 5 to 23.8 mg/g), error values for the hidden units are calculated, and their weights are changed. The backward propagation starts at the output layer and moves backward through the hidden layers until it reaches the input layer [73]. Table **1** presents the transfer functions at both the hidden and output layer used to optimize the model.

2.4. Error Analysis

The goodness of fit of the isotherm models to the experimental data was evaluated using the coefficient of determination, (R^2), as well as the Marquardt's Percent Standard Deviation (MPSD), Hybrid Error Function (HYBRID), Relative Percent Error (RPE) and Mean Square Error (MSE) which are presented in Table **2**.

3. RESULTS AND DISCUSSION

3.1. Equilibrium Analysis

The experimental equilibrium data which describes the adsorption of Cr(VI) by activated carbon was fitted to the two-parameter Langmuir [30] and Freundlich isotherms [31] as well as the three-parameter Sips isotherm [39], the original BET (Type 1) isotherm [69] and the modified BET (Type 2) isotherm [70]. Non-linear regression was used to simulate the experimental data, and the goodness of fit was assessed using error function the results of which are presented in Table **3**. Among these isotherm models, the Langmuir model produced the lowest error value.

The shape of the experimental curve (Fig. **2**) reveals similar characteristics as the classical Type II and Type IV BET isotherms and class 3 Giles L-shape isotherm (Fig. **3a-c**), where the flat region of the curve corresponds to the possible formation of a monolayer. Beyond this plateau, the curve begins to climb indicating the possible formation of multi-layers. A plot of the experimental isotherm data together with both Langmuir and modified BET model simulation are shown in Fig. (**2**). The Langmuir model produced the lowest error values; however, observations of the figure show that the model fails to properly capture the essence of the curve. Although the modified BET also failed to capture the shape of the experimental isotherm, a study of (Fig. **2**) reveals the modified BET sorption capacity, q_{mBET2} from Table **3** was successful in predicting the monolayer coverage of 18.08 mg/g. Though this can prove useful in comparing the performance of adsorbent in terms of monolayer coverage, the model cannot be used for performance and design predictions.

Table 1. Transfer Function.

Name of Transfer Function	Algorithm
logsig	$f(n) = 1/ (1 + exp(-n))$
tansig	$f(n) = [2/ (1 + exp(- 2*n))] -1$
purelin	$f(n) = n$

Table 2. Error functions.

Error Functions	Expression	Equation Number
Relative Percent Error (RPE)	where, N is the number of experimental points.	$RPE\% = \frac{1}{N}\sum_{i=1}^{N}\frac{\left[\left\|\left(q_{e_i}\right)_{pred} - \left(q_{e_i}\right)_{\exp}\right\|\right]}{\left(q_{e_i}\right)_{\exp}} * 100$ **(7)**
Marquardt's Percent Standard Deviation (MPSD)	where, N is the number of experimental points and P is the number of parameters in the regression model.	$MPSD = 100\sqrt{\frac{1}{N-P}\sum_{i=1}\left[\frac{(q_{ei})_{\exp} - (q_{ei})_{pred}}{(q_{ei})_{\exp}}\right]^2}$ **(8)**
The Hybrid Error Function (HYBRID)	where, N is the number of experimental points and P is the number of parameters in the regression model.	$HYBRID = \frac{100}{N-P}\sum_{i=1}^{N}\left[\frac{((q_{ei})_{\exp} - (q_{ei})_{pred})^2}{(q_{ei})_{pred}}\right]$ **(9)**
R^2	where, N is the number of experimental points.	$R^2 = \frac{\sum_{i=1}^{N}\left((q_{e_i})_{\exp} - q_{e_{exp,mean}}\right)^2 - \sum_{i=1}^{N}\left((q_{e_i})_{\exp} - (q_{e_i})_{pred}\right)^2}{\sum_{i=1}^{N}\left((q_{e_i})_{\exp} - (q_{e_i})_{pred}\right)^2}$ **(10)**
MSE	where, N is the number of experimental points.	$MSE = \left(\frac{1}{N}\sum_{i=1}^{N}\left[\left(q_{e_i}\right)_{\exp} - \left(q_{e_i}\right)_{pred}\right]^2\right)$ **(11)**

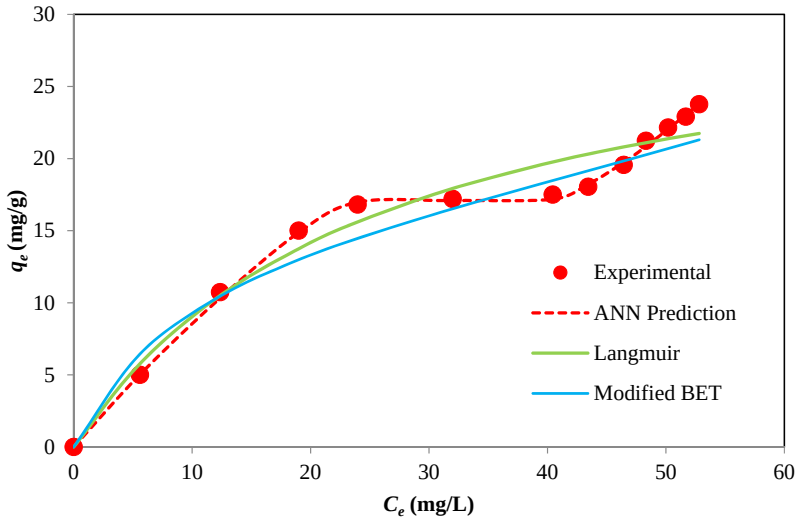

Fig. (2). Simulation of experimental data by isotherm models and ANN model.

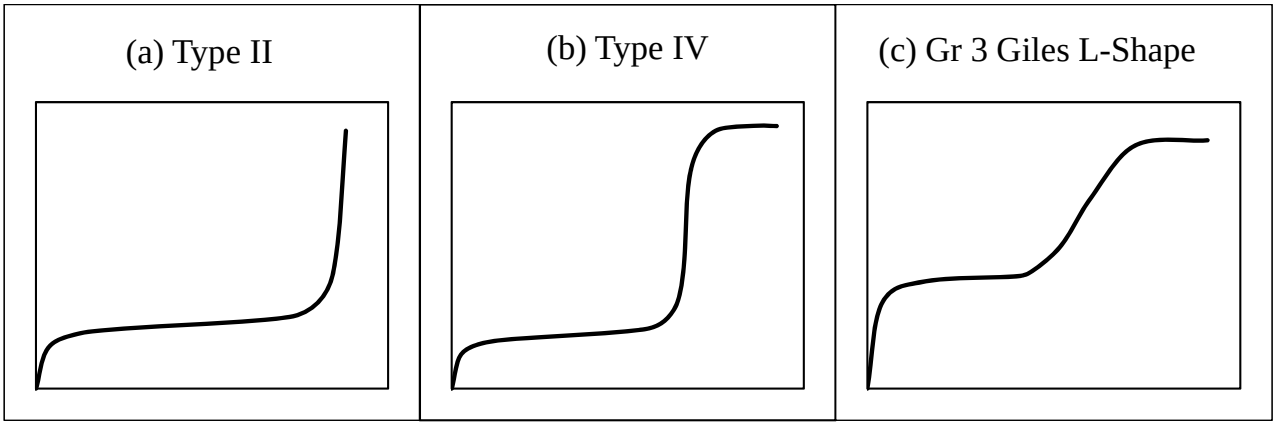

Fig. (3). Isotherm classifications: (**a**) BET Type II [19]; (**b**) BET Type IV [19]; and (**c**) Group 3 Giles L-shape isotherm [20].

Table 3. Comparison of isotherm and ANN models using non-linear regression for Cr(VI) uptake by activated carbon.

Model	Parameters	Error Functions		
		RPE	MPSD	HYBRID
Langmuir	q_e = 32.3; K_L = 0.039	10.991	12.098	21.441
Freundlich	K_F = 2.874; n = 1.94	13.446	19.325	32.299
Sips	q_s = 35.15; α_s = 0.032; n_s = 0.924	11.419	14.250	26.836
Original BET	q_{mBET1} = -18.05; K_b = 1.0628; C_s = -11.34	11.480	17.320	28.892
Modified BET	q_{mBET2} = 18.08; K_s = 0.0937; K_L = 0.0055	13.221	17.608	34.570
ANN		1.688	2.061	0.603

Table 4. Performance of varying training algorithms of ANN model.

Backpropagation (BP) Algorithms	Function	MSE	IN	R^2	Best Linear Eq.
BFGS quasi-Newton backpropagation	trainbfg	0.1098	2	0.7007	y=0.96x-0.51
Bayesian regularization BP	trainbr	0.0003	28	-	-
Powell–Beale conjugate gradient backpropagation	traincgb	0.0035	15	0.9853	y=1.0x-0.05

Backpropagation (BP) Algorithms	Function	MSE	IN	R^2	Best Linear Eq.
Fletcher–Reeves conjugate gradient backpropagation	traincgf	0.5197	69	0.8834	y=0.93x+0.17
Polak-Ribiere conjugate gradient BP	traincgp	0.0604	1	0.5004	y=0.98x+0.11
Gradient descent	traingd	0.0949	1000	0.9525	y=1.1x-0.13
Gradient descent with momentum	traingdm	0.1909	9	0.6791	y=0.84x-0.35
Gradient descent with adaptive learning rate	traingda	0.0020	39	0.8731	y=1.0x-0.077
Gradient descent with momentum & Adaptive Learning	traingdx	0.8794	24	0.7412	y=1.0x-0.03
Levenberg–Marquardt backpropagation	trainlm	0.0367	5	0.8626	y=1.1x-0.14
One step secant backpropagation	trainoss	0.2171	6	0.8542	y=0.8x+0.064
Random weight/Bias	trainr	0.1585	5	0.8044	y=0.82x+0.18
Resilient backpropagation	trainrp	0.0040	5	0.8991	y=0.81x-0.1
Scaled conjugate gradient backpropagation	trainscg	0.1957	2	0.8092	y=0.79x+0.24

3.2. Artificial Neural Network Model

An ANN model was developed and optimized in this study [using the neural network toolbox of MATLAB 7.14.0 (R2012a)®] to predict and simulate the equilibrium manner of Cr(VI) adsorption by activated carbon. A three layer feed-forward back propagation ANN model was adopted with an input layer comprising one neuron as residual concentration (C_e), while the output layer is the adsorbed solid concentration (q_e) (Table **6**). Critical to the performance of an ANN model is the design of its structure. Thus a protocol was developed for its optimization and is presented.

The data were first normalized in the range -1 to 1 using Eq. (12). The dataset was then divided whereby 85% of the data was applied to training the network and 15% for testing the accuracy of the model and its prediction.

$$X_{norm} = 2\left[\frac{X_i - X_{min}}{X_{max} - X_{min}}\right] - 1 \qquad \textbf{(12)}$$

Where:

X_i =input or output variable X

X_{min} = minimum value of variable X

The impact of training function on the network was first examined Table **4**. Using the tansig and purelin transfer functions at the hidden and output layer, respectively and 10 neurons at the hidden layer, the Bayesian regularization back-propagation algorithm produced the lowest MSE of 0.0003. Using the Bayesian regularization back-propagation algorithm, transfer functions from Table **1** were then varied to determine the impact on the network. The performance of these transfer functions at the hidden and output layers was assessed using the MSE and coefficient of determination. Using the first two training, the optimum functions were found to be a tangent sigmoid transfer function (tansig) at the hidden layer and a linear transfer function (purelin) at the output layer (Table **5**).

The number of nodes in the hidden layer is critical to the performance of the ANN model. Too few neurons can lead to under-fitting while too many neurons may result in over-fitting [74]. In this protocol, the number of nodes was varied up to 18 and its impact on performance assessed using the MSE. Fig. (**4**) presents the relationship between MSE value and the number of nodes in the hidden layer. The minimum MSE was found to be 0.00004 at neuron 10. Using this optimized network, the output is compared to the target value and presented in Fig. (**5**). The plot reveals a coefficient of determination of 0.9984 which is greater than 0.95 and as such, is acceptable. The optimum ANN structure is presented in Table **6**. Using the error functions presented in Table **2**, the precision of the simulation was assessed as shown in Table **3**. The prediction produced the lowest RPE, HYBRID, and MPSD as compared to the other standard equilibrium models. Though the model gives no insight into the mechanisms of adsorption, it does provide a useful tool for the prediction of sorption performance.

Table 5. Performance of varying transfer functions on ANN model.

Activation Function Layer 1	Activation Function Layer 2	MSE (First Training)	MSE (Second Training)	R^2 (First Training)	R^2 (Second Training)
Logsig	Logsig	0.1009	0.1190	-	-
Logsig	Purelin	0.0004	0.0004	0.9449	0.9449
Logsig	Tansig	0.0007	0.0057	0.993	0.993
Purelin	Logsig	0.3575	0.1661	0.9429	0.9429
Purelin	Purelin	0.0536	0.0506	0.9429	0.9429
Purelin	Tansig	0.1187	0.083	0.9411	0.9411
Tansig	Logsig	0.1307	0.1287	0.8487	0.8487
Tansig	Purelin	0.0003	0.0003	0.9995	0.9995
Tansig	Tansig	0.0403	0.0496	0.9296	0.9296

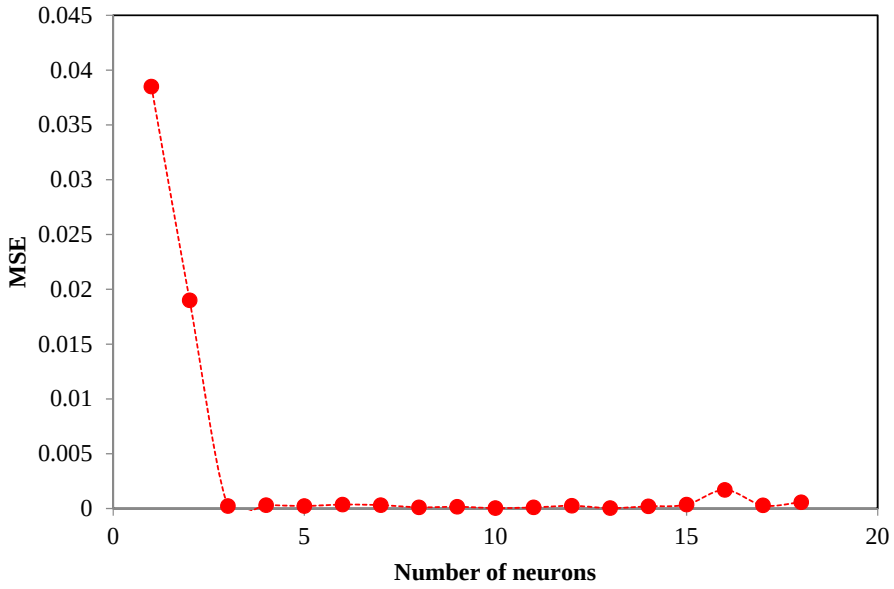

Fig. (4). Relationship between MSE and number of neurons at hidden layer.

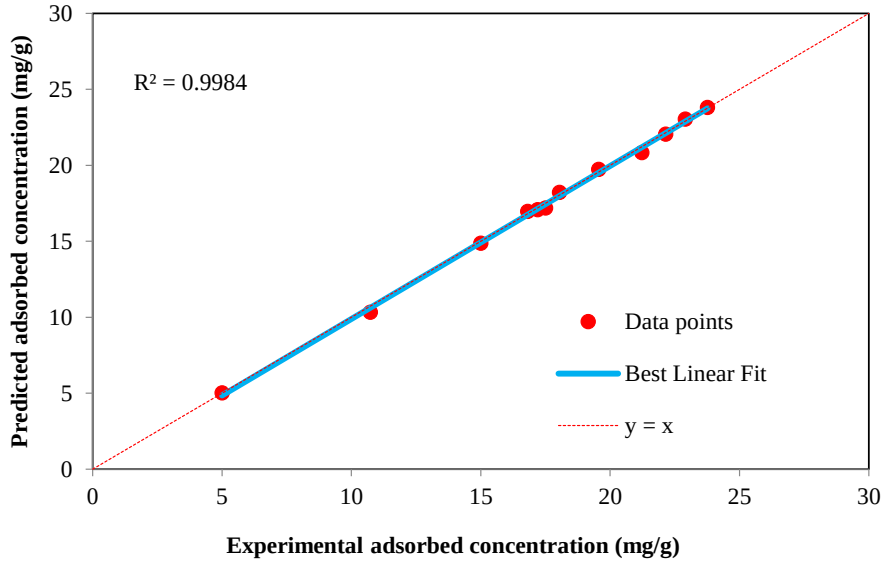

Fig. (5). Plot of ANN outputs *vs*. the corresponding experimental targets.

Table 6. Optimum ANN structure for equilibrium data.

Type	Details
Network type	Feed-forward backpropagation
Transfer function (Hidden Layer)	Tansig
Transfer function (Output Layer)	Purelin
Training function	Bayesian Regulation
Performance function	Mean Square Error (MSE)
Neurons in input layer	1
Neurons in hidden layer	10

(Table 6) contd.....

Type	Details
Neurons in output layer	1
Data used for training	85%
Data for testing	15%
R^2	0.9984

Table 7. Comparison of adsorption capacities of Cr(VI)with adsorbents reported in the literature.

Adsorbents	Monolayer Adsorption Capacity (mg/g)	pH	Reference
ZeoliteNaX	6.414	4	[75]
Jordanian pottery materials	28.8	3	[76]
Olive stone activated carbon	25.6	1.5	[77]
Pine needles	40	3	[78]
Ore	15.67	2	[79]
Clay	14.43	2	[79]
Magnetic-poly(divinylbenzene-vinylimidazole) microbeads	4.353	2	[80]
Activated carbon	18.08	2.5	This study

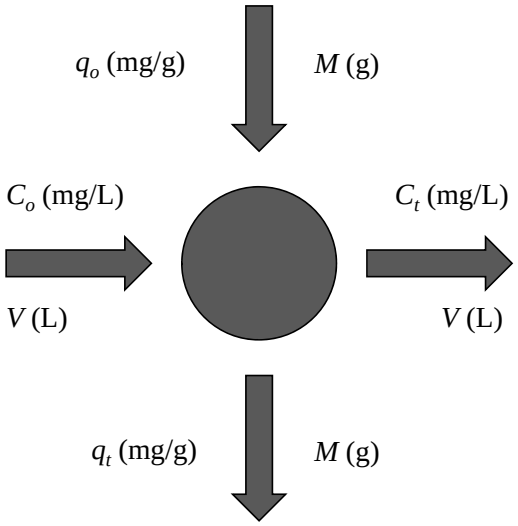

Fig. (6). Design of single-stage batch system for Cr(VI) adsorption.

3.3. Monolayer Comparison to Values in the Literature

The monolayer adsorption capacity of sorbents reported in the literature is compared in Table **7** to values obtained in this study. The table reveals that the activated carbon used in this study compares well to sorbents previously reported. It is noted that the adsorbent in this study exhibited characteristics of the multi-layer formation, which, within the range of operational parameters produced a maximum sorption capacity of 18.08 mg/g. Further, it is emphasized that the present study aims to predict the complex equilibrium behaviour of this adsorbent for the design of batch adsorbers.

3.4. Design of Batch Adsorption System from ANN Predicted Equilibrium Data

3.4.1. Theory of Batch Adsorbers

Laboratory-scale equilibrium studies are used to predict batch adsorber size and performance. Fig. (**6**) shows the schematic of a single-stage batch adsorber with a solution volume of V (L) and the initial Cr(VI) concentration, C_o is reduced to C_t as the reaction proceeds. The Cr(VI) loading on the adsorbent in the reactor of mass M (g), changes from q_o to q_t with increased reaction time. The mass balance for the reactor is given by the following [81, 82]:

$$V\,(C_0 - C_t) = M\,(q_t - q_0) = M\,q_t \qquad \textbf{(13)}$$

3.4.2. Development of a Predictive Model

An empirical equation was developed to predict adsorption capacity without having to run the ANN model in Matlab. This will be beneficial not only in saving cost and time required for experimental studies but also in improving the efficient application of full-scale adsorption systems [51]. The equation derived using the weights (W_i) and biases (b_i) to the input layer of the optimized network Table **8** is presented here as follows:

$$q_{e\ pred}=1.0969+0.94959F_2+1.2592F_3+0.30953F_4-0.12308F_5+0.02505F_6-0.038107F_7 +0.2706F_8+0.26463F_9+0.40543F_{10}+0.36964 \quad (14)$$

Where, coefficients are the weights and bias to the output layer and F_i is the tansig activation function used in the hidden layer and is given as:

$$F_i = \frac{2}{[1+\exp(-2*E_i)]} - 1 \quad ; i = 1{:}10 \quad (15)$$

And E_i is the weighted sum of the input defined as:

$$E_i = W_{i1} * C_e + b_i \quad (16)$$

3.4.3. Design of a Batch Adsorber

The adsorption process was best represented by the ANN model, thus the mass balance (Eq. 13) under equilibrium condition ($C_t \rightarrow C_e$ and $q_t \rightarrow q_e$) is arranged as follows:

$$\frac{M}{V} = \frac{C_0-C_e}{q_e} = \frac{C_o-C_e}{1.0969+0.94959F_2+1.2592F_3+0.30953F_4-0.12308F_5+0.02505F_6-0.038107F_7+ 0.2706F_8+0.26463F_9+0.40543F_{10}+0.36964} \quad (17)$$

Table 8. Weight and bias values obtained by the Bayesian Regularization BP algorithm with 10 neurons.

i	Input 1	Bias 1	Output
Node 1	3.1831	-3.7416	1.0969
Node 2	4.6201	-3.3772	0.9496
Node 3	-2.7785	2.0832	1.2592
Node 4	3.2129	-0.9658	0.3095
Node 5	3.0881	-0.3451	-0.1231
Node 6	-3.0856	-0.3557	0.0251
Node 7	-3.0853	-1.0384	-0.0381
Node 8	3.0822	1.7335	0.2706
Node 9	3.0794	2.4138	0.2646
Node 10	3.0795	3.0982	0.4054
Bias 2			0.3696

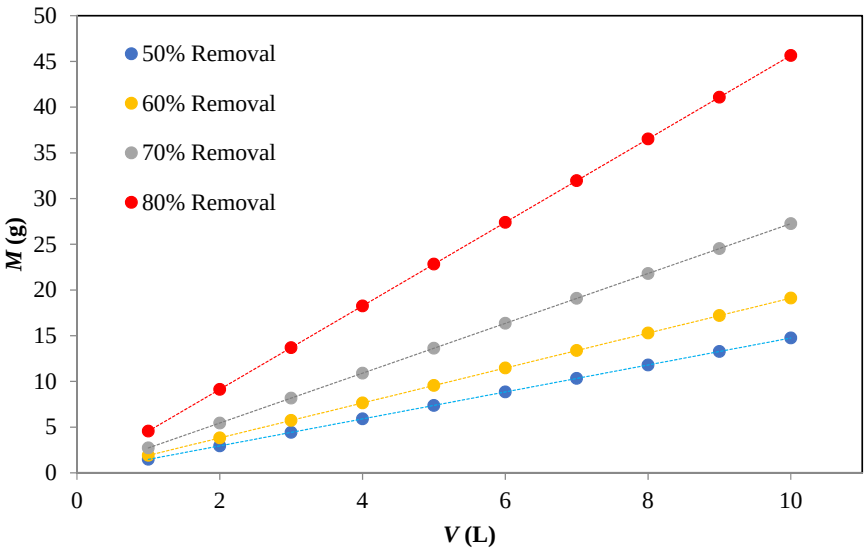

Fig. (7). Adsorbent mass (*M*) *vs* Volume of Cr(VI) solution treated (*V*).

Fig. (**7**) presents a series of plots of the predicted values of *M* (g) *versus V* (L) for 50%, 60%, 70% and 80% Cr(VI) ion removal at the initial concentration of 50 mg/L. As an example, the mass of adsorbent required for 70% Cr(VI) removal from aqueous solution was 8 g and 19 g, for Cr(VI) solution volumes of 3 L and 7, respectively. This evaluation becomes relevant for pilot-batch system design as well as large-scale batch applications.

CONCLUSION

The equilibrium data were modelled using classical two- and three-parameter isotherm models. Among these models, the Langmuir model produced the closest simulation to the experimental data; however, the model failed to successfully capture the shape of the isotherm. The modified BET model was successful in predicting the monolayer sorption capacity of the activated carbon for the Cr(VI) ions; however, the model also produced a poor simulation making it incapable for design applications. An ANN model was successfully developed to simulate and predict the experimental adsorption equilibrium data using the Bayesian Regulation training algorithm. The model was successfully applied to design batch absorbers which can enable up-scale to pilot and full-scale design.

CONSENT FOR PUBLICATION

Not applicable.

AVAILABILITY OF DATA AND MATERIALS

All data supporting the findings are included in the article.

FUNDING

None.

CONFLICT OF INTEREST

The authors declare no conflict of interest, financial or otherwise.

ACKNOWLEDGEMENTS

Declared none.

REFERENCES

[1] H. Oliveira, "Chromium as an environmental pollutant: Insights on induced plant toxicity", *J. Bot.,* vol. 2012, 2012. [http://dx.doi.org/10.1155/2012/375843]

[2] D.S. Thambavani, and B. Kavitha, "Prediction and simulation of Chromium (VI) ions removal efficiency by riverbed sand adsorbent using Artificial Neural Networks", *Int. J. Eng. Sci. Res. Technol,* vol. 3, no. 5, pp. 906-913, 2014.

[3] M. Pazos, M. Branco, I.C. Neves, M.A. Sanromán, and T. Tavares, "Removal of Cr(VI) from aqueous solutions by a bacterial biofilm supported on zeolite: Optimisation of the operational conditions and scale-Up of the bioreactor", *Chem. Eng. Technol.,* vol. 33, no. 12, pp. 2008-2014, 2010. [http://dx.doi.org/10.1002/ceat.201000203]

[4] A. Bhattacharya, A. Gupta, A. Kaur, and D. Malik, "Alleviation of hexavalent chromium by using microorganisms: Insight into the strategies and complications", *Water Sci. Technol.,* vol. 79, no. 3, pp. 411-424, 2019. [http://dx.doi.org/10.2166/wst.2019.060] [PMID: 30924796]

[5] V. Velma, S.S. Vutukuru, and P.B. Tchounwou, "Ecotoxicology of hexavalent chromium in freshwater fish: A critical review", *Rev. Environ. Health,* vol. 24, no. 2, pp. 129-145, 2009. [http://dx.doi.org/10.1515/REVEH.2009.24.2.129] [PMID: 19658319]

[6] K. Mubeena, and G. Muthuraman, "Extraction and stripping of Cr(VI) from aqueous solution by solvent extraction", *Desalin. Water Treat.,* vol. 55, no. 8, pp. 2201-2208, 2015. [http://dx.doi.org/10.1080/19443994.2014.930697]

[7] P. Mishra, and R. Soni, "Analysis of dyeing and printing waste water of Balotara textile industries", *Int. J. Chem. Sci.,* vol. 14, no. 4, pp. 1929-1938, 2016.

[8] N. Tara, M. Arslan, Z. Hussain, M. Iqbal, Q.M. Khan, and M. Afzal, "On-site performance of floating treatment wetland macrocosms augmented with dye-degrading bacteria for the remediation of textile industry wastewater", *J. Clean. Prod.,* vol. 217, pp. 541-548, 2019. [http://dx.doi.org/10.1016/j.jclepro.2019.01.258]

[9] D. Krishna, and R. Sree, "Artificial Neural Network (ANN) approach for modeling chromium (VI) adsorption from aqueous solution using a Borassus flabellifer coir powder", *Int. J. Appl. Sci. Eng,* vol. 12, no. 3, pp. 177-192, 2014.

[10] C. Sutherland, and C. Venkobachar, "A diffusion-chemisorption kinetic model for simulating biosorption using forest macro-fungus Fomes fasciatus", *Int. Res. J. Pl. Sci.,* vol. 1, pp. 107-117, 2010.

[11] S. Goswami, and U.C. Ghosh, "Studies on adsorption behaviour of Cr(VI) onto synthetic hydrous stannic oxide", *Water S.A.,* vol. 31, no. 4, pp. 597-602, 2005.

[12] A. Alemu, B. Lemma, N. Gabbiye, M.T. Alula, and M.T. Desta, "Removal of chromium (VI) from aqueous solution using vesicular basalt: A potential low cost wastewater treatment system", *Heliyon,* vol. 4, no. 7, pp. 1-22, 2018. [http://dx.doi.org/10.1016/j.heliyon.2018.e00682]

[13] D. Kučić, M. Simonič, and L. Furač, "Batch adsorption of Cr(VI) ions on zeolite and agroindustrial waste", *Chem. Biochem. Eng. Q.,* vol. 31, no. 4, pp. 497-507, 2017. [http://dx.doi.org/10.15255/CABEQ.2017.1100]

[14] T.V. Reddy, S. Chauhan, and S. Chakraborty, "Adsorption isotherm and kinetics analysis of hexavalent chromium and mercury on mustard oil cake", *Environ. Eng. Res.,* vol. 22, no. 1, pp. 95-107, 2016. [http://dx.doi.org/10.4491/eer.2016.094]

[15] T. Srinath, T. Verma, P.W. Ramteke, and S.K. Garg, "Chromium (VI) biosorption and bioaccumulation by chromate resistant bacteria", *Chemosphere,* vol. 48, no. 4, pp. 427-435, 2002. [http://dx.doi.org/10.1016/S0045-6535(02)00089-9] [PMID: 12152745]

[16] D. Duranoğlu, and U. Beker, "Cr(VI) adsorption onto biomass waste material-derived activated carbon", in Desalination Updates. IntechOpen, 2015, pp. 273-302. [http://dx.doi.org/10.5772/60206]

[17] C. Sutherland, and C. Venkobachar, "Equilibrium modeling of Cu (II) biosorption onto untreated and treated forest macro-fungus Fomes fasciatus", *Int. J. Plant Anim. Environ. Sci.,* vol. 3, pp. 193-203, 2013.

[18] C. Ng, J.N. Losso, W.E. Marshall, R.M. Rao, and R. Marshall, "Freundlich adsorption isotherms of agricultural by-product-based powdered activated carbons in a geosmin-water system", *Bioresour. Technol.,* vol. 85, no. 2, pp. 131-135, 2002. [http://dx.doi.org/10.1016/S0960-8524(02)00093-7] [PMID: 12227536]

[19] S. Brunauer, L.S. Deming, W.E. Deming, and E. Teller, "On a theory of the van der Waals adsorption of gases", *J. Am. Chem. Soc.,* vol. 62, no. 7, pp. 1723-1732, 1940. [http://dx.doi.org/10.1021/ja01864a025]

[20] C.H. Giles, A.P. D'Silva, and I.A. Easton, "A general treatment and classification of the solute adsorption isotherm part. II. Experimental interpretation", *J. Colloid Interface Sci.,* vol. 47, no. 3, pp. 766-778, 1974. [http://dx.doi.org/10.1016/0021-9797(74)90253-7]

[21] A.R. Netzahuatl-Muñoz, Mdel.C. Cristiani-Urbina, and E. Cristiani-Urbina, "Chromium biosorption from Cr(VI) aqueous solutions by Cupressus lusitanica bark: Kinetics, equilibrium and thermodynamic studies", *PLoS One,* vol. 10, no. 9, 2015.e0137086 [http://dx.doi.org/10.1371/journal.pone.0137086] [PMID: 26352933]

[22] P. Terangpi, S. Chakraborty, and M. Ray, "Improved removal of hexavalent chromium from 10 mg/L solution by new micron sized polymer clusters of aniline formaldehyde condensate", *Chem. Eng. J.,* vol. 350, pp. 599-607, 2018. [http://dx.doi.org/10.1016/j.cej.2018.05.171]

[23] Z. Sfaksi, N. Azzouz, and A. Abdelwahab, "Removal of Cr(VI) from water by cork waste", *Arab. J. Chem.,* vol. 7, no. 1, pp. 37-42, 2014. [http://dx.doi.org/10.1016/j.arabjc.2013.05.031]

[24] A. De Rossi, M.R. Rigon, M. Zaparoli, R.D. Braido, L.M. Colla, G.L.

Dotto, and J.S. Piccin, "Chromium (VI) biosorption by Saccharomyces cerevisiae subjected to chemical and thermal treatments", *Environ. Sci. Pollut. Res. Int.,* vol. 25, no. 19, pp. 19179-19186, 2018. [http://dx.doi.org/10.1007/s11356-018-2377-4] [PMID: 29808404]

[25] M.M. El-Halwany, "Kinetics and thermodynamics of activated Sunflowers Seeds Shell Carbon (SSSC) as sorbent material", *J. Chromatogr. Sep. Tech.,* vol. 4, pp. 5-11, 2013. [http://dx.doi.org/10.4172/2157-7064.1000183]

[26] T. Sismanoglu, A. Ercag, S. Pura, and E. Ercag, "Kinetics and isotherms of dazomet adsorption on natural adsorbents", *J. Braz. Chem. Soc.,* vol. 15, no. 5, pp. 669-675, 2004. [http://dx.doi.org/10.1590/S0103-50532004000500010]

[27] S. Álvarez-Torrellas, M. Martin-Martinez, H.T. Gomes, G. Ovejero, and J. García, "Enhancement of p-nitrophenol adsorption capacity through N2-thermal-based treatment of activated carbons", *Appl. Surf. Sci.,* vol. 414, pp. 424-434, 2017. [http://dx.doi.org/10.1016/j.apsusc.2017.04.054]

[28] D. Zhang, Y. Ma, H. Feng, and Y. Hao, "Adsorption of Cr(VI) from aqueous solution using carbon-microsilica composite adsorbent", *J. Chil. Chem. Soc.,* vol. 57, no. 1, pp. 964-968, 2012. [http://dx.doi.org/10.4067/S0717-97072012000100002]

[29] R. Ramadoss, and D. Subramaniam, "Adsorption of chromium using blue green algae-modeling and application of various isotherms", *Int. J. Chem. Technol.,* vol. 10, pp. 1-22, 2018. [http://dx.doi.org/10.3923/ijct.2018.1.22]

[30] I. Langmuir, "The adsorption of gases on plane surface of glass, mica and platinum", *J. Am. Chem. Soc.,* vol. 40, pp. 1361-1368, 1916. [http://dx.doi.org/10.1021/ja02242a004]

[31] H.M.F. Freundlich, "Over the adsorption in solution", *J. Phys. Chem.,* vol. 57, pp. 385-470, 1906.

[32] L. Jossens, J.M. Prausnitz, W. Fritz, E.U. Schlunder, and A.L. Myers, "Thermodynamics of multi-solute adsorption from dilute aqueous solutions", *Chem. Eng. Sci.,* vol. 33, pp. 1097-1106, 1978. [http://dx.doi.org/10.1016/0009-2509(78)85015-5]

[33] R.H. Fowler, and E.A. Guggenheim, *Statistical Thermodynamics.,* Cambridge University Press: London, England, 1939.

[34] M.I. Temkin, "Adsorption equilibrium and process kinetics on homogeneous surfaces and with interaction between adsorbed molecules", *Zh Fiz Khim.,* vol. 15, pp. 296-332, 1941.

[35] O. Redlich, and D.L. Peterson, "A useful adsorption isotherm", *J. Phys. Chem.,* vol. 63, pp. 1024-1026, 1959. [http://dx.doi.org/10.1021/j150576a611]

[36] C.J. Radke, and J.M. Prausnitz, "Adsorption of organic solutes from dilute aqueous solution of activated carbon", *Ind. Eng. Chem. Fund,* vol. 11, pp. 445-451, 1972.

[37] R.A. Koble, and T.E. Corrigan, "Adsorption isotherms for pure hydrocarbons", *Ind. Eng. Chem.,* vol. 44, pp. 383-387, 1952. [http://dx.doi.org/10.1021/ie50506a049]

[38] J. Toth, "State equation of the solid-gas interface layers", *Acta Chir. Hung.,* vol. 69, pp. 311-328, 1971.

[39] R. Sips, "On the structure of a catalysts surface", *J. Chem. Phys.,* vol. 16, pp. 490-495, 1948. [http://dx.doi.org/10.1063/1.1746922]

[40] A.R. Khan, R. Ataullah, and A. Al-Haddad, "Equilibrium adsorption studies of some aromatic pollutants from dilute aqueous solutions on activated carbon at different temperatures", *J. Colloid Interface Sci.,* vol. 194, no. 1, pp. 154-165, 1997. [http://dx.doi.org/10.1006/jcis.1997.5041] [PMID: 9367594]

[41] M. Baudu, Etude des interactions solutes-fibres de charbon actif: Applications et regeneration", Ph.D. Thesis, University in Rennes, France, 1990.

[42] B.M. Van Vliet, W.J. Weber Jr, and H. Hozumi, "Modeling and prediction of specific compound adsorption by activated carbon and synthetic adsorbents", *Water Res.,* vol. 14, pp. 1719-1728, 1980. [http://dx.doi.org/10.1016/0043-1354(80)90107-4]

[43] W. Fritz, and E.U. Schluender, "Simultaneous adsorption equilibria of organic solutes in dilute aqueous solutions on activated carbon", *Chem. Eng. Sci.,* vol. 29, pp. 1279-1282, 1974. [http://dx.doi.org/10.1016/0009-2509(74)80128-4]

[44] F.R.C. Pedroza, M.D.J.S. Aguilar, M.A.S. Castillo, A.M. Luévanos, and N.G.P. Rodríguez, "Adsorption of chromium from steel plating wastewater using blast furnace dust", *Rev. Int. Contam. Ambient.,* vol. 33, no. 4, pp. 591-603, 2017. [http://dx.doi.org/10.20937/RICA.2017.33.04.04]

[45] M. Schneider, A. Drenkova-Tuhtan, W. Szczerba, C. Gellermann, C. Meyer, H. Steinmetz, K. Mandel, and G. Sextl, "Nanostructured ZnFeZr oxyhydroxide precipitate as efficient phosphate adsorber in waste water: Understanding the role of different material-building-blocks", *Environ. Sci. Nano,* vol. 4, no. 1, pp. 180-190, 2017. [http://dx.doi.org/10.1039/C6EN00507A]

[46] Z. Al-Qodah, and R. Shawabkah, "Production and characterization of granular activated carbon from activated sludge", *Braz. J. Chem. Eng.,* vol. 26, no. 1, pp. 127-136, 2009. [http://dx.doi.org/10.1590/S0104-66322009000100012]

[47] D. Gnanasangeetha, and D.S. Thambavani, "Modelling and biosorption competence of zinc oxide nanoparticle", *Nat. Environ. Pollut. Technol.,* vol. 14, no. 2, pp. 41-44, 2015.

[48] W.S. McCulloch, and W. Pitts, "A logical calculus of the ideas immanent in nervous activity. 1943", *Bull. Math. Biol.,* vol. 52, no. 1-2, pp. 99-115, 1990. [http://dx.doi.org/10.1007/BF02459570] [PMID: 2185863]

[49] J.D. Olden, and D.A. Jackson, "Illuminating the "black box": A randomization approach for understanding variable contributions in artificial neural networks", *Ecol. Modell.,* vol. 154, no. 1-2, pp. 135-150, 2002. [http://dx.doi.org/10.1016/S0304-3800(02)00064-9]

[50] Q.H. Gong, J.X. Zhang, and J. Wang, "Application of GIS-Based back propagation artificial neural networks and logistic regression for shallow landslide susceptibility mapping in south china-take meijiang river basin as an example", *Open Civ. Eng. J.,* vol. 12, pp. 21-34, 2018. [http://dx.doi.org/10.2174/1874149501812010021]

[51] G. Naja, V. Diniz, and B. Volesky, "Predicting metal biosorption performance", STL Harrison, DE Rawlings, and J. Peterson, Eds., *Proceedings of the 16th International Bio-hydrometallurgy Symposium,* 2005, pp. 553-562

[52] B. Tarawneh, W.A. Bodour, and K.A. Ajmi, "Intelligent computing based formulas to predict the settlement of shallow foundations on cohesionless soils", *Open Civ. Eng. J.,* vol. 13, no. 1, 2019. [http://dx.doi.org/10.2174/1874149501913010001]

[53] K. Gopalakrishnan, "Neural networks analysis of airfield pavement heavy weight deflectometer data", *Open Civ. Eng. J.,* vol. 2, pp. 15-23, 2008. [http://dx.doi.org/10.2174/1874149500802010015]

[54] B.S. Chittoo, and C. Sutherland, "Phosphate removal and recovery using lime-iron sludge: adsorption, desorption, fractal analysis, modeling and optimization using artificial neural network-genetic algorithm", *Desalin. Water Treat.,* vol. 63, pp. 227-240, 2017. [http://dx.doi.org/10.5004/dwt.2017.20195]

[55] A.M. Ghaedi, M. Ghaedi, A.R. Pouranfard, A. Ansari, Z. Avazzadeh, A. Vafaei, I. Tyagi, S. Agarwal, and V.K. Gupta, "Adsorption of triamterene on multi-walled and single-walled carbon nanotubes: Artificial neural network modeling and genetic algorithm optimization", *J. Mol. Liq.,* vol. 216, pp. 654-665, 2016. [http://dx.doi.org/10.1016/j.molliq.2016.01.068]

[56] K. Yetilmezsoy, and S. Demirel, "Artificial Neural Network (ANN) approach for modeling of Pb(II) adsorption from aqueous solution by Antep pistachio (Pistacia Vera L.) shells", *J. Hazard. Mater.,* vol. 153, no. 3, pp. 1288-1300, 2008. [http://dx.doi.org/10.1016/j.jhazmat.2007.09.092] [PMID: 17980484]

[57] M.R. Fagundes-Klen, P. Ferri, T.D. Martins, C.R.G. Tavares, and E.A. Silva, "Equilibrium study of the binary mixture of cadmium–zinc ions biosorption by the Sargassum filipendula species using adsorption isotherms models and neural network", *Biochem. Eng. J.,* vol. 34, no. 2, pp. 136-146, 2007. [http://dx.doi.org/10.1016/j.bej.2006.11.023]

[58] C. Sutherland, A. Marcano, and B. Chittoo, Artificial neural network-genetic algorithm prediction of heavy metal removal using a novel plant-based biosorbent banana floret: Kinetic, equilibrium, thermodynamics and desorption studies*Desalin. Water Trea.*. M. Eyvaz and E. Yüksel, IntechOpen, **2018**, pp. 385-411 [http://dx.doi.org/10.5772/intechopen.74398]

[59] K.M. Desai, S.A. Survase, P.S. Saudagar, S.S. Lele, and R.S. Singhal, "Comparison of Artificial Neural Network (ANN) and Response Surface Methodology (RSM) in fermentation media optimization: Case study of fermentative production of scleroglucan", *Biochem. Eng. J.,* vol. 41, no. 3, pp. 266-273, 2008. [http://dx.doi.org/10.1016/j.bej.2008.05.009]

[60] F. Karimi, S. Rafiee, A. Taheri-Garavand, and M. Karimi, "Optimization of an air drying process for Artemisia absinthium leaves using response surface and artificial neural network models", *J. Taiwan Inst. Chem. Eng.,* vol. 43, no. 1, pp. 29-39, 2012. [http://dx.doi.org/10.1016/j.jtice.2011.04.005]

[61] K. Kadirvelu, M. Palanival, R. Kalpana, and S. Rajeswari, "Activated

carbon from an agricultural by-product, for the treatment of dyeing industry wastewater", *Bioresour. Technol.,* vol. 74, no. 3, pp. 263-265, 2000.
[http://dx.doi.org/10.1016/S0960-8524(00)00013-4]

[62] R. Tovar-Gómez, M.R. Moreno-Virgen, J.A. Dena-Aguilar, V. Hernández-Montoya, A. Bonilla-Petriciolet, and M.A. Montes-Morán, "Modeling of fixed-bed adsorption of fluoride on bone char using a hybrid neural network approach", *Chem. Eng. J.,* vol. 228, pp. 1098-1109, 2013.
[http://dx.doi.org/10.1016/j.cej.2013.05.080]

[63] D.S. Lee, C.O. Jeon, J.M. Park, and K.S. Chang, "Hybrid neural network modeling of a full-scale industrial wastewater treatment process", *Biotechnol. Bioeng.,* vol. 78, no. 6, pp. 670-682, 2002.
[http://dx.doi.org/10.1002/bit.10247] [PMID: 11992532]

[64] M.A. Hussain, M.S. Rahman, and C.W. Ng, "Prediction of pores formation (porosity) in foods during drying: Generic models by the use of hybrid neural network", *J. Food Eng.,* vol. 51, no. 3, pp. 239-248, 2002.
[http://dx.doi.org/10.1016/S0260-8774(01)00063-2]

[65] H. Pfost, and V. Headley, "Methods of determining and expressing particle size", *Feed Manuf. Technol,* pp. 512-517, 1976.

[66] C. Sutherland, B.S. Chittoo, and C. Venkobachar, "A comparative study of hybrid artificial neural network models for predicting Cr(VI) adsorption onto activated carbon", *Desalination Water Treat.,* vol. 103, pp. 182-198, 2018.
[http://dx.doi.org/10.5004/dwt.2018.21930]

[67] US Environmental Protection Agency (USEPA), "Fate, transport, and transformation test guidelines. Adsorption/desorption", OPPTS 835.1230, Washington, DC, 2008.

[68] E. Swan, and A.R. Urquhart, "Adsorption equations a review of the literature", *J. Phys. Chem.,* vol. 31, pp. 251-276, 1927.
[http://dx.doi.org/10.1021/j150272a008]

[69] S. Brunauer, P.H. Emmet, and E. Teller, "Adsorption of gases in multimolecular layers", *J. Am. Chem. Soc.,* vol. 60, pp. 309-319, 1938.
[http://dx.doi.org/10.1021/ja01269a023]

[70] A. Ebadi, J.S. Soltan Mohammadzadeh, and A. Khudiev, "What is the correct form of BET isotherm for modeling liquid phase adsorption?", *Adsorp.,* vol. 15, no. 1, pp. 65-73, 2009.
[http://dx.doi.org/10.1007/s10450-009-9151-3]

[71] G. Morse, R. Jones, J. Thibault, and F.H. Tezel, "Neural network modeling of adsorption isotherms", *Adsorp.,* vol. 17, no. 2, pp. 303-309, 2011.
[http://dx.doi.org/10.1007/s10450-010-9287-1]

[72] S. Lek, and J.F. Guegan, "Artificial neural networks as a tool in ecological modeling, an introduction", *Ecol. Modell.,* vol. 120, pp. 65-73, 1999.
[http://dx.doi.org/10.1016/S0304-3800(99)00092-7]

[73] M. Bean, and C. Jutten, "Neural networks in geophysical applications", *Geophysics,* vol. 65, pp. 1032-1047, 2000.
[http://dx.doi.org/10.1190/1.1444797]

[74] K. Yetilmezsoy, "Modeling studies for the determination of completely mixed activated sludge reactor volume: Steady-state, empirical and ANN applications", *Neural Netw. World,* vol. 20, pp. 559-589, 2010.

[75] P.K. Pandey, S.K. Sharma, and S.S. Sambi, "Kinetics and equilibrium study of chromium adsorption on zeoliteNaX", *Int. J. Environ. Sci. Technol.,* vol. 7, no. 2, pp. 395-404, 2010.
[http://dx.doi.org/10.1007/BF03326149]

[76] K. Al-Sou'od, "Adsorption isotherm studies of chromium (VI) from aqueous solutions using Jordanian pottery materials", *APCBEE Proc,* vol. 1, 2012pp. 116-125
[http://dx.doi.org/10.1016/j.apcbee.2012.03.020]

[77] A.A. Attia, S.A. Khedr, and S.A. Elkholy, "Adsorption of chromium ion (VI) by acid activated carbon", *Braz. J. Chem. Eng.,* vol. 27, no. 1, pp. 183-193, 2010.
[http://dx.doi.org/10.1590/S0104-66322010000100016]

[78] M.R. Hadjmohammadi, M. Salary, and P. Biparva, "Removal of Cr(VI)from aqueous solution using pine needles powder as a biosorbent", *J. App. Sci. Environ. Santi,* vol. 6, no. 1, 2011.

[79] A. Ksakas, A. Loqman, B. El Bali, M. Taleb, and A. Kherbeche, "The adsorption of Cr(VI) from aqueous solution by natural materials", *J. Mater. Environ. Sci.,* vol. 6, no. 7, pp. 2003-2012, 2015.

[80] A. Kara, and E. Demirbel, "Kinetic, isotherm and thermodynamic analysis on adsorption of Cr(VI) ions from aqueous solutions by synthesis and characterization of magnetic-poly (divinylbenzene-vinylimidazole) microbeads", *Water Air Soil Pollut.,* vol. 223, no. 5, pp. 2387-2403, 2012.
[http://dx.doi.org/10.1007/s11270-011-1032-1] [PMID: 22707803]

[81] G. McKay, M.S. Otterburn, and J.A. Aga, "Fuller's earth and fired clay as adsorbents for dyestuffs", *Water Air Soil Pollut.,* vol. 24, no. 3, pp. 307-322, 1985.
[http://dx.doi.org/10.1007/BF00161790]

[82] F. Deniz, "Dye removal by almond shell residues: Studies on biosorption performance and process design", *Mater. Sci. Eng. C,* vol. 33, no. 5, pp. 2821-2826, 2013.
[http://dx.doi.org/10.1016/j.msec.2013.03.009] [PMID: 23623102]